

Coherent population transfer between weakly-coupled states in a ladder-type superconducting qutrit

H. K. Xu,¹ W. Y. Liu,¹ G. M. Xue,¹ F. F. Su,¹ H. Deng,¹ Ye Tian,¹ D. N. Zheng,¹
Siyuan Han,^{2,1} Y. P. Zhong,³ H. Wang,³ Yu-Xi Liu,⁴ and S. P. Zhao¹

¹*Beijing National Laboratory for Condensed Matter Physics,
Institute of Physics, Chinese Academy of Sciences, Beijing 100190, China*

²*Department of Physics and Astronomy, University of Kansas, Lawrence, KS 66045, USA*

³*Department of Physics, Zhejiang University, Hangzhou 310027, China*

⁴*Institute of Microelectronics, Tsinghua University, Beijing 100084, China*

Stimulated Raman adiabatic passage (STIRAP) offers significant advantages for coherent population transfer between un- or weakly-coupled states and has the potential of realizing efficient quantum gate, qubit entanglement, and quantum information transfer. Here we report on the realization of STIRAP in a superconducting phase qutrit - a ladder-type system in which the ground state population is coherently transferred to the second-excited state via the dark state subspace. The result agrees well with the numerical simulation of the master equation, which further demonstrates that with the state-of-the-art superconducting qutrits the transfer efficiency readily exceeds 99% while keeping the population in the first-excited state below 1%. We show that population transfer via STIRAP is significantly more robust against variations of the experimental parameters compared to that via the conventional resonant π pulse method. Our work opens up a new venue for exploring STIRAP for quantum information processing using the superconducting artificial atoms.

PACS numbers:

Stimulated Raman adiabatic passage (STIRAP), which combines the processes of stimulated Raman scattering and adiabatic passage, is a powerful tool used for coherent population transfer (CPT) between un- or weakly-coupled quantum states^{1,2}. It has been recognized as an important technique in quantum computing and circuit QED involving superconducting qubits³⁻¹². For example, qubit rotations can be realized via STIRAP with the two computational states plus an auxiliary state forming a three-level Λ configuration^{3,4}. A scheme for generating arbitrary rotation and entanglement in the three-level Λ -type flux qutrits is also proposed⁵, and the experimental feasibility of realizing quantum information transfer and entanglement between qubits inside microwave cavities has been discussed^{6,7}. Unlike the conventional resonant π pulse method STIRAP is known to be much more robust against variations in experimental parameters, such as the frequency, amplitude, and interaction time of microwave fields, and the environmental noise^{4,5,10,11}.

Recently, multi-level systems (qutrits or qudits) have found important applications in speeding up quantum gates¹³, realizing quantum algorithms¹⁴, simulating quantum systems consisting of spins greater than $1/2$ ¹⁵, implementing full quantum-state tomography¹⁶⁻¹⁸, and testing quantum contextuality¹⁹. Unlike the highly anharmonic Λ -type flux qutrits the phase and transmon qutrits have the ladder-type (Ξ -type) three-level configuration which is weakly anharmonic. The dipole coupling between the ground state $|0\rangle$ and the second-excited state $|2\rangle$ in the phase qutrit is much weaker than those between the first-excited state $|1\rangle$ and the $|0\rangle$ state or the $|2\rangle$ state. In the case of the transmon qutrit the coupling is simply zero. This unique property makes it difficult to transfer population from $|0\rangle$ to $|2\rangle$ directly using a single π pulse tuned to their level spacing ω_{20} . The usual solution is to use the high-power resonant two-photon process or to apply two successive π pulses transferring the population first from

$|0\rangle$ to $|1\rangle$ and then from $|1\rangle$ to $|2\rangle$ ^{17,18}. These methods often lead to a significant population in the middle level $|1\rangle$ resulting in energy relaxation which degrades the transfer process. In contrast, STIRAP transfers the qutrit population directly from $|0\rangle$ to $|2\rangle$ via the dark state subspace without occupying the middle level $|1\rangle$.

In this work, we report on the realization of STIRAP in a Ξ -type superconducting phase qutrit²⁰. As shown schematically in Fig. 1a the qutrit has a loop inductance L and a Josephson junction with critical current I_c and capacitance C . The potential energy and quantized levels $|0\rangle$, $|1\rangle$, and $|2\rangle$ of the qutrit are illustrated in Fig. 1b in which the frequencies $\omega_{p,s}$ of the pump and Stokes fields and their strength $\Omega_{p,s}$ (Rabi frequencies) are also indicated. Applying the rotating-wave approximation (RWA) in the double-rotating frame the Hamiltonian of the system can be written as^{21,22}:

$$H = \begin{bmatrix} 0 & g_p + g_s e^{-i\delta t} & 0 \\ g_p + g_s e^{i\delta t} & \Delta_p & \lambda(g_p e^{i\delta t} + g_s) \\ 0 & \lambda(g_p e^{-i\delta t} + g_s) & \Delta_p + \Delta_s \end{bmatrix}, \quad (1)$$

where the Planck constant \hbar is set to unity, $\delta = \omega_p - \omega_s$, $\Delta_p = \omega_{10} - \omega_p$ and $\Delta_s = \omega_{21} - \omega_s$ are various detunings, $g_{p,s}$ are the qutrit-microwave couplings proportional to the amplitude of the pump and Stokes fields respectively, and $\lambda \approx \sqrt{2}$ for the Ξ -type configuration with weak anharmonicity. For $\delta \gg \Omega_{p,s}$ the fast-oscillating terms in equation (1) averages out to zero so the Hamiltonian becomes

$$H' = \begin{bmatrix} 0 & \Omega_p/2 & 0 \\ \Omega_p/2 & \Delta_p & \Omega_s/2 \\ 0 & \Omega_s/2 & \Delta_p + \Delta_s \end{bmatrix}, \quad (2)$$

in which $\Omega_p = 2g_p$ and $\Omega_s = 2\lambda g_s$. For the phase qutrit used here we have $\lambda \approx 1.45$. Equation (2) is the well-known RWA Raman Hamiltonian^{1,2}. In particular, when the system

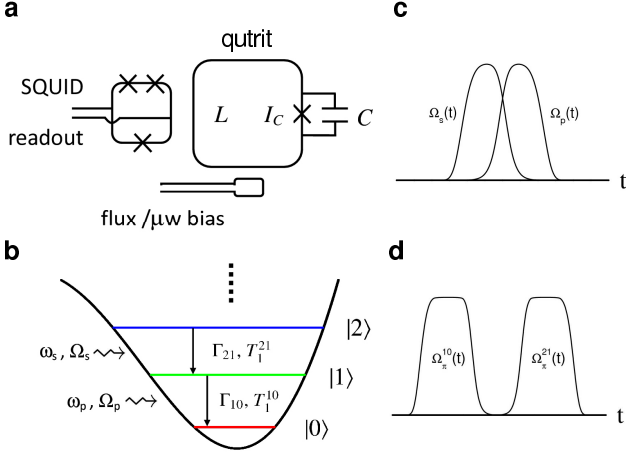


FIG. 1: Superconducting phase qutrit and measurement pulse sequences. (a) Schematic rf-SQUID type phase qutrit with Josephson critical current I_c , shunt capacitance C , and loop inductance L . (b) Three bottom energy levels $|0\rangle$, $|1\rangle$, and $|2\rangle$ of the qutrit with related symbols indicated. Subscripts p and s refer to the pump and Stokes tones, respectively. (c) Counterintuitive pulse sequence with Ω_s preceding Ω_p for coherent population transfer from $|0\rangle$ to $|2\rangle$ without involving $|1\rangle$. (d) Conventional resonant π pulse sequence for successive $|0\rangle \rightarrow |1\rangle \rightarrow |2\rangle$ population transfers.

satisfies the two-photon resonant condition:

$$\Delta_p + \Delta_s = 0, \quad (3)$$

it has an eigenstate $|D\rangle = \cos \Theta |0\rangle - \sin \Theta |2\rangle$, called the dark state, which corresponds to the eigenvalue of $\epsilon = 0$. Here $\tan \Theta(t) = \Omega_p(t)/\Omega_s(t)$. CPT from the ground state $|0\rangle$ to the second-excited state $|2\rangle$ without populating the first-excited state $|1\rangle$ can therefore be realized via STIRAP by initializing the qutrit in the ground state $|0\rangle$ ^{22,23} and then slowly increasing the ratio $\Omega_p(t)/\Omega_s(t)$ to infinity as long as the following conditions^{1,2,24,25}

$$\delta \gg \Omega_{p,s}, \text{ and } \int_{-\infty}^{\infty} \sqrt{\Omega_p^2(t) + \Omega_s^2(t)} dt > 10\pi \quad (4)$$

are satisfied so that the qutrit will stay in the dark state subspace spanned by $\{|0\rangle, |2\rangle\}$. The first condition is required to reduce equation (1) to equation (2) leading to the existence of the dark state solution while the second ensures adiabatic state following.

Results

Sample parameters and measurements. The sample used in this work is an aluminum phase qutrit²⁰, which is cooled down to $T \approx 10$ mK in an Oxford cryogen-free dilution refrigerator. The qutrit control and measurement circuit includes various filtering, attenuation, and amplification²⁶. For the present experiment, we bias the rf-SQUID to have six energy levels in the upper potential well and use the lowest three levels as the qutrit states. The relevant transition frequencies are $f_{10} = \omega_{10}/2\pi = 5.555$ GHz and $f_{21} = \omega_{21}/2\pi = 5.393$ GHz, and the relative anharmonicity is $\alpha = (f_{10} - f_{21})/f_{10} \approx 2.9\%$.

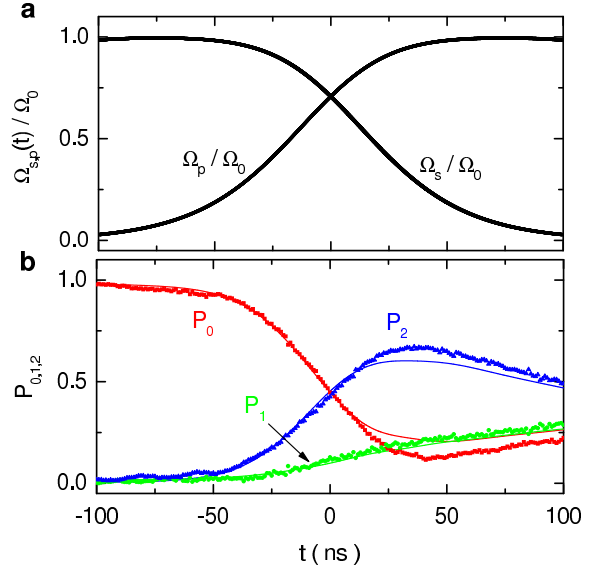


FIG. 2: Coherent population transfer via STIRAP in the superconducting phase qutrit. (a) Stokes and pump microwave pulses $\Omega_s(t)$ and $\Omega_p(t)$ shown in the overlapped region with the experimental parameters $\Omega_0/2\pi = 42.8 \pm 1.0$ MHz and $T_d = 100$ ns. (b) Level populations P_0 , P_1 , and P_2 versus time in the case of $\Delta_p = \Delta_s = 0$. A maximum experimental value of $P_2 = 67\%$, limited by the low decoherence times of the device, is reached. Experimental and calculated results are shown as symbols and lines, respectively.

The measured energy relaxation times are $T_1^{10} = 1/\Gamma_{10} = 353$ ns and $T_1^{21} = 1/\Gamma_{21} = 196$ ns, respectively, while the dephasing time determined from Ramsey interference experiment is $T_\varphi^{10} = 124$ ns. To realize STIRAP, a pair of bell-shaped counterintuitive microwave pulses with the Stokes pulse preceding the pump pulse, as illustrated in Fig. 1c, are used. The pulses are defined by $\Omega_s(t) = \Omega_0 F(t) \cos[\pi f(t)/2]$ and $\Omega_p(t) = \Omega_0 F(t) \sin[\pi f(t)/2]$ with $F(t) = e^{-(t/2T_d)^6}$ and $f(t) = 1/(1 + e^{-4t/T_d})^{2,25}$. The pulse width (FWHM) is approximately $2T_d$, and its height is $0.967\Omega_0$, and $\Omega_s(0) = \Omega_p(0)$.

Coherent population transfer. Figure 2a shows the two microwave pulses defined by $\Omega_0/2\pi = 42.8 \pm 1.0$ MHz and $T_d = 100$ ns in their overlapping region. As t increases, $\Omega_s(t)$ and $\Omega_p(t)$ start to increase and decrease across $t = 0$ at which they are equal. The experimentally measured populations P_0 , P_1 , and P_2 versus time produced by this counterintuitive pulse sequence in the resonant case $\Delta_p = \Delta_s = 0$ are plotted in Fig. 2b as symbols. We observe that as time evolves across $t = 0$ the population P_2 (P_0) increases (decreases) rapidly, signifying the occurrence of STIRAP via the dark state of the superconducting qutrit system. The experimentally achieved maximum P_2 , or the population transfer efficiency, is about 67% for the present sample under the resonant condition. Notice that in the entire region of $t \in [-100, 100]$ ns, all of the characteristic features of the experimental data, in particular (i) P_1 remaining significantly lower than P_2 for $t > -50$ ns, (ii) the decrease (increase) of P_2 (P_0) after reaching the maximum (minimum) as well as the gradual rising of P_1 , are reproduced well by the numerical simulation (solid lines). The simulated tempo-

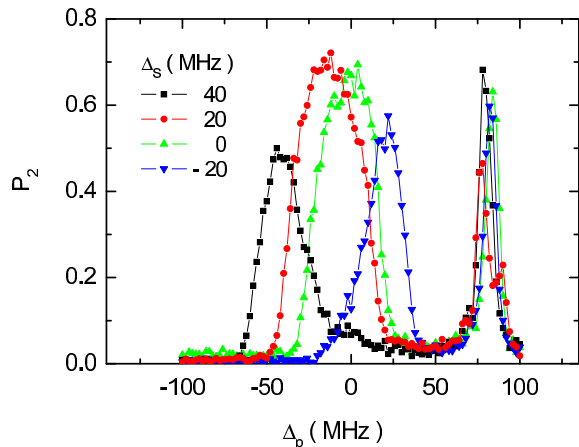


FIG. 3: **Level population P_2 versus pump microwave detuning Δ_p for four Stokes tone detunings.** Bright resonances can be seen as the resonant condition equation (3) is satisfied (left-side peaks in each curves). A maximum value of $P_2 = 72\%$ is reached at the microwave detunings $\Delta_p = -\Delta_s = -20$ MHz. The right-side peaks result from the two-photon process of the single pump microwave tone.

ral profiles of the populations P_0 , P_1 , and P_2 are obtained by solving the master equation $\dot{\rho} = -(i/\hbar)[H, \rho] + L(\rho)$, using the measured qutrit parameters, where $L(\rho)$ is the Liouvillian containing the relaxation and dephasing processes²². The numerical result also confirms that feature (ii) is due primarily to energy relaxation, while the maximum P_2 itself is mainly limited by dephasing. Hence by increasing the qutrit decoherence times the undesirable decrease of P_2 and the rise of P_1 and P_0 in the relevant time scale can be suppressed and a higher P_2 can be achieved (see below).

In our experiment the conditions imposed by equation (4) are satisfied: $\delta/2\pi$ in the resonant case $\Delta_p = \Delta_s = 0$ is $f_{10} - f_{21} = 162$ MHz, which is approximately four times that of $\Omega_0/2\pi$, and it is easy to verify that the integrated pulse area $\int_{-\infty}^{\infty} \sqrt{\Omega_p^2(t) + \Omega_s^2(t)} dt \approx 32\pi$ is greater than 10π . In addition to reducing decoherence the efficiency of the demonstrated STIRAP process can be improved by increasing the relatively small anharmonicity parameter $\alpha \approx 2.9\%$ of the present sample up to, say, 10% by optimizing device parameters of the Ξ -type phase and transmon (or Xmon) qutrits^{27,28}. According to equation (4) greater anharmonicity allows the use of larger Ω_0 which would proportionally reduce the duration of the pump and Stokes pulses when the pulse area is kept unchanged to satisfy the adiabatic condition. Shorter pulses also reduce the negative effect of decoherence on the transfer efficiency.

The STIRAP process is often identified in either the time domain or the frequency domain^{1,2}. The latter is based on equation (3) which specifies the two-photon resonance condition. In Fig. 3, we show the level $|2\rangle$ population P_2 versus the pump detuning Δ_p for four Stokes tone detunings of $\Delta_s = 40, 20, 0$, and -20 MHz, respectively. Bright resonance appears as the left-side peak in each curve when the two-photon resonant condition equation (3) is met. It is interesting to see that the maximum value of $P_2 = 72\%$ is reached at the microwave detunings of $\Delta_p = -\Delta_s = -20$ MHz,

which is higher than the value achieved in the resonant case of $\Delta_p = \Delta_s = 0$ shown in Fig. 2b. In Fig. 3, the right-side peak in each curve is originated from the two-photon process excited by the single pump microwave tone. Compared to the left-side peaks, although the peak heights are comparable, they are much narrower, indicating that in practice it is less controllable using the two-photon process to perform coherent population transfer from state $|0\rangle$ to state $|2\rangle$.

Efficiency and robustness. The above results demonstrate clearly CPT from the ground state $|0\rangle$ to the second-excited state $|2\rangle$ via STIRAP in the Ξ -type superconducting qutrit. Compared to the usual high-power two-photon process or two non-overlapping successive resonant π pulse excitations shown in Fig. 1d, which involve significant undesired population in the middle level $|1\rangle$ and require precise single photon resonance and pulse area^{10,17}, CPT via STIRAP demonstrates just the opposite. First, in principle CPT between $|0\rangle$ and $|2\rangle$ can be accomplished without occupying the lossy middle level $|1\rangle$. More importantly, the process is much more robust against variations in the frequency, duration, and shape of the driving pulses^{1,2}. In fact, in terms of the conditions equation (3) and equation (4), we see from Fig. 3 that the single photon resonance condition is greatly relaxed. Although $\Omega_{p,s}$ are limited by the system anharmonicity, their values, together with T_d , still have much room for variations while maintaining the transfer efficiency.

In Fig. 4a, we show the calculated results in the Ω_0 versus T_d plane with contours indicating population transfer efficiency above 99% and 98%, respectively, using qutrits with decoherence times of $T_1^{10} = 35.3 \mu\text{s}$, $T_1^{21} = 19.6 \mu\text{s}$, and $T_\phi^{10} = 12.4 \mu\text{s}$, and the relative anharmonicity of $\alpha = 8\%$. The qutrit parameters in the ranges are now attainable with transmon^{28,29}, Xmon³⁰, flux³¹, and also possibly phase²⁷ type devices. In Fig. 4b, we show the level populations versus time (solid lines) for $\Omega_0/2\pi = 100$ MHz and $T_d = 50$ ns, in which a nearly complete transfer above 99% from level $|0\rangle$ to level $|2\rangle$ is accomplished with the population in middle level $|1\rangle$ kept below 1%. These results indicate that the transfer efficiency of STIRAP is very insensitive to Ω_0 , which is limited by systems anharmonicity, and to T_d , which should be much smaller than the decoherence time. The allowed variations of a few hundreds of MHz in Ω_0 and a few tens of ns in T_d for keeping $P_2 > 99\%$, for example, are in sharp contrast with the case of simple π pulse excitations. In fact, using a π pulse to transfer population from the ground state $|0\rangle$ to the first-excited state $|1\rangle$ alone, acceptable variations of the Rabi frequency Ω and pulse width T to keep the transfer efficiency above 99% can be estimated from the pulse area relation $\Omega \times T \approx (1 \pm 0.06)\pi$. Thus if we use $\Omega/2\pi = 50$ MHz, the pulse width variation must be less than ± 0.6 ns. More strict condition is required when successive excitation from the first-excited state $|1\rangle$ to the second-excited state $|2\rangle$ is considered. From these we see that the extreme robustness of the STIRAP process is very advantageous and should be useful in various applications such as realizing efficient qubit rotation, entanglement, and quantum information transfer in various superconducting qubit and qutrit systems.

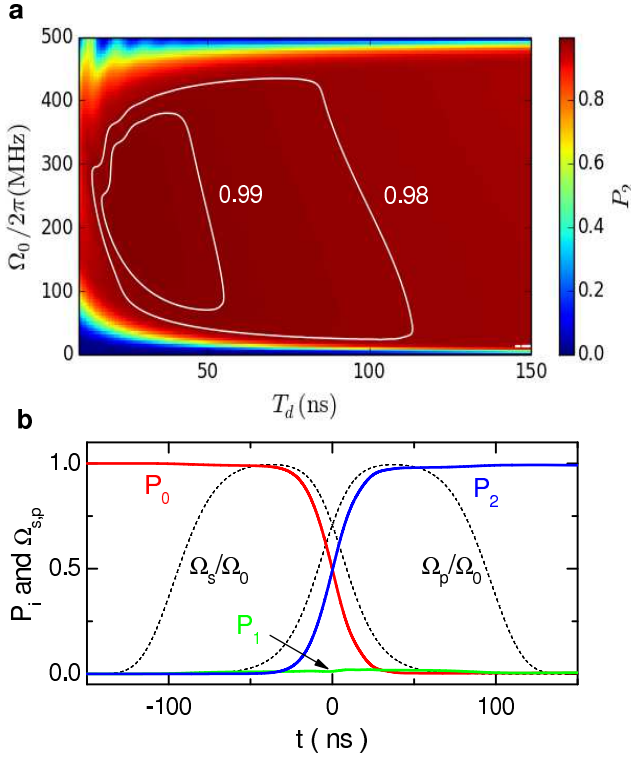


FIG. 4: **Calculated results demonstrating the robustness of the STIRAP process.** (a) Results in the Ω_0 versus T_d plane with contours for population transfer efficiency above 99% and 98% indicated. The same sample parameters as those in Fig. 2b are used in the calculation but the decoherence times are increased to $T_1^{10} = 35.3 \mu\text{s}$, $T_1^{21} = 19.6 \mu\text{s}$, and $T_\varphi^{10} = 12.4 \mu\text{s}$ and the relative anharmonicity to $\alpha = 8\%$. (b) The temporal profiles of microwave pulses (dashed lines) and level populations (solid lines) in the case of $\Omega_0/2\pi = 100$ MHz and $T_d = 50$ ns.

Discussion

We have experimentally demonstrated coherent population transfer between two weakly-coupled states, $|0\rangle$ and $|2\rangle$, of a superconducting phase qutrit having the Ξ -type ladder configuration via STIRAP. The qutrit had a small relative anharmonicity of 2.9%, and moderate decoherence times of $T_\varphi^{10} = 124$ ns, $T_1^{10} = 353$ ns, and $T_1^{21} = 196$ ns, respectively. We demonstrated that by applying a pair of counterintuitive microwave pulses in which the Stokes tone precedes the pump tone, coherent population transfer from $|0\rangle$ to $|2\rangle$ with a 72% efficiency can be achieved with a much smaller population in the first-excited state $|1\rangle$. Using the measured qutrit parameters, including decoherence times, we simulated the STIRAP process by numerically solving the master equation. The result agrees well with the experimental data. We showed that by increasing the decoherence times of the qutrits to the order of a few tens of microseconds, currently attainable experimentally, the transfer efficiency can be increased to greater than 99% while keeping the population of the first-excited state below 1%.

We have also shown that coherent population transfer via STIRAP is much more robust against variations of the

experimental parameters, including the amplitude, detuning, and time duration of the microwave fields, and the environmental noise over the conventional methods such as using high-power two-photon excitation and two resonant π pulses tuned to ω_{10} and ω_{21} , respectively. Therefore STIRAP is advantageous for achieving robust coherent population transfer in the ladder-type superconducting artificial atoms that play increasingly important roles in various fields ranging from fundamental physics to quantum information processing. Furthermore, the method can be readily extended to the Λ -type systems such as the superconducting flux qutrits, in which the initial and target states locate in different potential wells representing circulating currents in opposite directions. Our work paves the way for further progress in these directions.

Methods

Determination of level populations. The qutrit level populations $P_i(t)$ ($i = 0, 1, 2$) at a given time t are determined using two carefully calibrated nanosecond-scale measurement flux pulses A and B, which reduce the potential barrier to two different levels so that tunneling probabilities p^A and p^B in each case are measured. Pulse A leads to low tunneling probability p_0^A ($\sim 5\%$) for state $|0\rangle$, high tunneling probability p_1^A for state $|1\rangle$ and, of course, even higher tunneling probability p_2^A for state $|2\rangle$. Pulse B results in a slightly deeper potential well than pulse A does so that $p_0^B \approx 0$, $p_1^B \approx 5\%$, and a much larger p_2^B for state $|0\rangle$, $|1\rangle$, and $|2\rangle$ respectively. Denoting the density operator of the qutrit as ρ , we have

$$P^{A,B} = P_0 p_0^{A,B} + P_1 p_1^{A,B} + P_2 p_2^{A,B}, \quad (5)$$

where $P_i = \rho_{ii}$, and $p_i^{A,B}$ can be found from the experimentally determined tunneling probabilities p_i of the i th energy level for given amplitudes of pulses A and B¹⁸. Combining the normalization condition

$$\text{Tr}\rho = P_0 + P_1 + P_2 = 1, \quad (6)$$

we obtain

$$P_i = [(p_j^B - p_k^B)p^A + (p_k^A - p_j^A)p^B + p_j^A p_k^B - p_k^A p_j^B] / D, \quad (7)$$

where $i = 0, 1, 2$ with $\{i, j, k\}$ in circulative order like $\{0, 1, 2\}$, $\{1, 2, 0\}$, and $\{2, 0, 1\}$, and D is the determinant

$$D = \begin{vmatrix} 1 & 1 & 1 \\ p_0^A & p_1^A & p_2^A \\ p_0^B & p_1^B & p_2^B \end{vmatrix}. \quad (8)$$

Hence the level populations P_0 , P_1 , and P_2 can be obtained by measuring p^A and p^B .

Numerical simulations. We numerically calculate the level populations $P_0(t) = \rho_{00}(t)$, $P_1(t) = \rho_{11}(t)$, and $P_2(t) = \rho_{22}(t)$ at any given time by solving the master equation

$$\dot{\rho} = -\frac{i}{\hbar}[H, \rho] + L(\rho), \quad (9)$$

where ρ is the system's 3×3 density matrix, H is the Hamiltonian given by equation (1), and $L(\rho)$ is the Liouvillian containing various relaxation and dephasing processes. Since experimentally the pump and Stokes microwaves are not correlated, we introduce a phase difference ϕ between the two

microwaves in the actual calculations³². In this case, the double-rotating reference frame is described by the operator $U = |0\rangle\langle 0| + |1\rangle\langle 1|e^{i\omega_p t} + |2\rangle\langle 2|e^{i(\omega_p t + \omega_s t - \phi)}$, and the rotating-

wave approximation leads to a Hamiltonian in the following form:

$$H = \begin{bmatrix} 0 & g_p + g_s e^{-i(\delta t - \phi)} & 0 \\ g_p + g_s e^{i(\delta t - \phi)} & \Delta_p & \lambda[g_p e^{i(\delta t - \phi)} + g_s] \\ 0 & \lambda[g_p e^{-i(\delta t - \phi)} + g_s] & \Delta_p + \Delta_s \end{bmatrix}, \quad (10)$$

where the Liouvillian operator in equation (9) is given by²²:

$$L(\rho) = -\frac{1}{2} \begin{bmatrix} -2\Gamma_{10}\rho_{11} & (\Gamma_{10} + \gamma_{10}^\varphi)\rho_{01} & (\Gamma_{21} + \gamma_{20}^\varphi)\rho_{02} \\ (\Gamma_{10} + \gamma_{10}^\varphi)\rho_{10} & 2\Gamma_{10}\rho_{11} - 2\Gamma_{21}\rho_{22} & (\Gamma_{10} + \Gamma_{21} + \gamma_{21}^\varphi)\rho_{12} \\ (\Gamma_{21} + \gamma_{20}^\varphi)\rho_{20} & (\Gamma_{10} + \Gamma_{21} + \gamma_{21}^\varphi)\rho_{21} & 2\Gamma_{21}\rho_{22} \end{bmatrix}. \quad (11)$$

We use the parameters $\Gamma_{10} = 2.83 \times 10^6 \text{ sec}^{-1}$, $\Gamma_{21} = 5.10 \times 10^6 \text{ sec}^{-1}$, and $\gamma_{10}^\varphi = 8.06 \times 10^6 \text{ sec}^{-1}$ measured directly from experiment, while from the measured dc Stark shift of the two-photon spectral lines we estimate $\gamma_{20}^\varphi \approx 2\gamma_{10}^\varphi$ and $\gamma_{21}^\varphi \approx \gamma_{10}^\varphi$. In our calculations $\rho(t, \phi)$ is obtained by solving equation (9) using the fourth-order Runge-Kutta method. Since the phase difference ϕ of the two microwaves in our experiment is ran-

dom, we average the result over ϕ and finally arrive at:

$$\rho(t) = \frac{1}{2\pi} \int_0^{2\pi} \rho(t, \phi) d\phi. \quad (12)$$

-
- ¹ Bergmann, K., Theuer, H. & Shore, B. W. Coherent population transfer among quantum states of atoms and molecules. *Rev. Mod. Phys.* **70**, 1003 (1998).
- ² Shore, B. W. *Manipulating Quantum Structures using Laser Pulses* (Cambridge University Press, Cambridge, 2011).
- ³ Zhou, Z. Y., Chu, S. I. & Han, S. Quantum computing with superconducting devices: A three-level SQUID qubit. *Phys. Rev. B* **66**, 054527 (2002).
- ⁴ Kis, Z. & Renzoni, F. Qubit rotation by stimulated Raman adiabatic passage. *Phys. Rev. A* **65**, 032318 (2002).
- ⁵ Kis, Z. & Paspalakis, E. Arbitrary rotation and entanglement of flux SQUID qubits. *Phys. Rev. B* **69**, 024510 (2004).
- ⁶ Yang, C. P., Chu, S. I. & Han, S. Possible realization of entanglement, logical gates, and quantum-information transfer with superconducting-quantum-interference-device qubits in cavity QED. *Phys. Rev. A* **67**, 042311 (2003).
- ⁷ Yang, C. P., Chu, S. I. & Han, S. Quantum information transfer and entanglement with SQUID qubits in cavity QED: a dark-state scheme with tolerance for nonuniform device parameter. *Phys. Rev. Lett.* **92**, 117902 (2004).
- ⁸ Zhou, Z. Y., Chu, S. I. & Han, S. Suppression of energy-relaxation-induced decoherence in Λ -type three-level SQUID flux qubits: a dark-state approach. *Phys. Rev. B* **70**, 094513 (2004).
- ⁹ Liu, Y. X., You, J. Q., Wei, L. F., Sun, C. P. & Nori, F. Optical selection rules and phase-dependent adiabatic state control in a superconducting quantum circuit. *Phys. Rev. Lett.* **95**, 087001 (2005).
- ¹⁰ Wei, L. F., Johansson, J. R., Cen, L. X., Ashhab, S. & Nori, F. Controllable coherent population transfers in superconducting qubits for quantum computing. *Phys. Rev. Lett.* **100**, 113601 (2008).
- ¹¹ Siewert, J., Brandes, T. & Falci, G. Advanced control with a Cooper-pair box: stimulated Raman adiabatic passage and Fock-state generation in a nanomechanical resonator. *Phys. Rev. B* **79**, 024504 (2009).
- ¹² Falci, G., La Cognata, A., Berritta, M., D'Arrigo, A., Paladino, E. & Spagnolo, B. Design of a Lambda system for population transfer in superconducting nanocircuits. *Phys. Rev. B* **87**, 214515 (2013).
- ¹³ Lanyon, B. P. *et al.* Simplifying quantum logic using higher-dimensional Hilbert spaces. *Nat. Phys.* **5**, 134 (2009).
- ¹⁴ DiCarlo, L. *et al.* Demonstration of two-qubit algorithms with a superconducting quantum processor. *Nature* **460**, 240 (2009).
- ¹⁵ Neeley, M. *et al.* Emulation of a quantum spin with a superconducting phase qubit. *Science* **325**, 722 (2009).
- ¹⁶ Thew, R. T., Nemoto, K., White, A. G. & Munro, W. J. Qudit quantum-state tomography. *Phys. Rev. A* **66**, 012303 (2002).
- ¹⁷ Bianchetti, R. *et al.* Control and tomography of a three level superconducting artificial atom. *Phys. Rev. Lett.* **105**, 223601 (2010).
- ¹⁸ Shalibo, Y. *et al.* Direct Wigner tomography of a superconducting anharmonic oscillator. *Phys. Rev. Lett.* **110**, 100404 (2013).
- ¹⁹ Cabello, A. *et al.* Proposed experiments of qutrit state-

- independent contextuality and two-qutrit contextuality-based non-locality. *Phys. Rev. A* **85**, 032108 (2012).
- ²⁰ Simmonds, R. W. *et al.* Decoherence in Josephson phase qubits from junction resonators. *Phys. Rev. Lett.* **93**, 077003 (2004).
- ²¹ Sillanpää, M. A. *et al.* Autler-Townes effect in a superconducting three-level system. *Phys. Rev. Lett.* **103**, 193601 (2009).
- ²² Li, J. *et al.* Decoherence, Autler-Townes effect, and dark states in two-tone driving of a three-level superconducting system. *Phys. Rev. B* **84**, 104527 (2011).
- ²³ Novikov, S. *et al.* Autler-Townes splitting in a three-dimensional transmon superconducting qubit. *Phys. Rev. B* **88**, 060503 (2013).
- ²⁴ Scully M. O. & Zubairy, M. S. *Quantum Optics* (Cambridge University Press, Cambridge, 1997).
- ²⁵ Vasilev, G. S., Kuhn, A. & Vitanov, N. V. Optimum pulse shapes for stimulated Raman adiabatic passage. *Phys. Rev. A* **80**, 013417 (2009).
- ²⁶ Tian, Y. *et al.* A cryogen-free dilution refrigerator based Josephson qubit measurement system. *Rev. Sci. Instrum.* **83**, 033907 (2012).
- ²⁷ Whittaker, J. D. *et al.* Tunable-cavity QED with phase qubits. *Phys. Rev. B* **90**, 024513 (2014).
- ²⁸ Hoi, I. C. *et al.* Giant cross-Kerr effect for propagating microwaves induced by an artificial atom. *Phys. Rev. Lett.* **111**, 053601 (2013).
- ²⁹ Paik, H. *et al.* Observation of high coherence in Josephson junction qubits measured in a three-dimensional circuit QED architecture. *Phys. Rev. Lett.* **107**, 240501 (2011).
- ³⁰ Barends, R. *et al.* Coherent Josephson qubit suitable for scalable quantum integrated circuits. *Phys. Rev. Lett.* **111**, 080502 (2013).
- ³¹ Stern, M. *et al.* Flux qubits with long coherence times for hybrid quantum circuits. *Phys. Rev. Lett.* **113**, 123601 (2014).
- ³² Li, J. *et al.* Dynamical Autler-Townes control of a phase qubit. *Sci. Rep.* **2**, 645 (2012).

Acknowledgements

We thank J. M. Martinis (UCSB) for providing us with the sample used in this work. This work was supported by the Ministry of Science and Technology of China (Grant Nos. 2011CBA00106, 2014CB921202, and 2015CB921104) and the National Natural Science Foundation of China (Grant Nos. 91321208 and 11161130519). S. Han acknowledges support by the US NSF (PHY-1314861).

Author contributions

H.K.X., S.H., and S.P.Z. designed the experiment. H.K.X., W.Y.L., G.M.X., and F.F.S. performed the measurement and numerical simulation. Y.T., H.D., D.N.Z., Y.P.Z., and H.W. contributed to the experiment in the low-temperature achievement, sample mounting and characterization. Y.X.L. provided theoretical support. S.P.Z. and S.H. wrote the manuscript in cooperation with all the authors.

Additional information

Competing financial interests: The authors declare no competing financial interests.